JOINT INSTITUTE FOR NUCLEAR RESEARCH
Frank Laboratory of Neutron Physics

Final report on coexistence of superconductivity and ferromagnetism at low-dimensional heterostructures

Supervisor
Dr. Vladimir Zhaketov

Student
Ibrahim Ahmed Ibrahim

Participation period
February 26 – April 14, 2024
Wave 10

Contents

Acknowledgement

Completing this research project would not have been possible without the support of my supervisor; Dr. Vladimir Zhaketov, Frank Laboratory of Neutron Physics, to whom I extend my heartfelt thanks for his valuable insights, guidance, and encouragement. Also, I would like to express my thanks for Joint Institute for Nuclear Research “Interest Program” for giving me this great opportunity to be a participant in wave 10.

Abstract

We investigated the coexistence of superconductivity and ferromagnetism at low dimensional heterostructures using MATLAB simulations of various nominal structures and the experimental technique of polarized neutron reflectometry through the REMUR spectrometer at JINR.

Additionally, we used numerical methods to study the changing properties of neutron and X-ray scattering from thickness, magnetization, and multiple layers. We talked about how the grazing angle of the neutron beam, colinear and non-collinear magnetization, the thickness of the ferromagnetic layer, various ferromagnetic materials, the size of the superlattice, and the roughness of the structure affect the reflectivity spectra because of the interaction of neutrons with nuclei and magnetic moments.

By contrasting the various values of the characteristics and various ferromagnetic materials, we may determine that there is a reciprocal influence.

1. Introduction

1.1 Proximity effects in superconductor-ferromagnet structures

Dutch physicist Heike Kamerlingh Onnes discovered the superconductivity phenomenon in 1911, It is the sudden disappearance of electrical resistance by cooling the material below a characteristic temperature called **critical temperature "Tc"** [1].

In 1986, several cuprite-oxide superconductors were discovered, including YBCO, $Bi_2Sr_2CaCu_2O_{8+\delta}$ (BSCCO), and HgTiBaCaCuO with critical temperatures beyond 77 K. In 1933, W. Meissner and R. Ochsenfeld found that superconducting materials expelled the magnetic field from its volume at or below Tc. In contrast, due to the magnetic induction effect, the realizable ferromagnet materials concentrate the field's force lines inside its volume.

As competing phenomena, superconducting and ferromagnetic coexist in uniform materials is complex. It requires unique and rugged conditions. Ginzburg [2] proposed the first explanation of the superconductivity suppression via ferromagnetic ordering in the transition metals. He indicated that in these metals, magnetic induction exceeds the critical field.

The proximity effect was defined by P. F. Dahl in 1984 [3] as the partial transfer of superconducting properties to a typical metal as they are connected electrically because of the large spatial extension of the wave function of the Cooper pairs at distances comparable with the coherence length. In contrast, the reverse proximity effect may occur in a ferromagnet (FM) superconductor (S) heterostructures, which implies magnetization of the superconducting layer. [4]

Studies of heterogeneous systems involving ferromagnetic and superconducting materials have been conducted extensively since the publication of the pioneering papers by Z. Radovic et al. [6] and Y.N. Proshin et al. [7] developing the fundamentals of the theory of FM/S junctions. The temperature dependence of the magnetic proximity effect is investigated in [8].

1.2 Polarized neutron reflectometry

Historically, polarized neutrons were used in the study of the magnetic properties of ferromagnets by neutron depolarization method where the polarization of the transmitted neutron beam through the sample was measured. Currently, neutron reflectometry is used on a larger scale for different investigations as magnetic excitations in ferromagnets, structures of magnetic materials, and investigation of solid body surfaces.[10]

Fundamentally, the theory behind neutron reflectometry is the scattering of scalar quantum particles with the potential function as the interaction potential between neutrons in the neutron beam and the materials constituting the sample [11].

The apparatus structure in figure 1 is essentially a reactor (source of neutrons), a polarizer (magnetic supermirrors, transmission through polarized gas as He, or transmission through magnetized films), a spin flipper (space varying magnetic field that is constant in time, a combination of radio frequency and constant fields), the sample, another spin flipper followed by a polarization analyzer, and finally a detector.

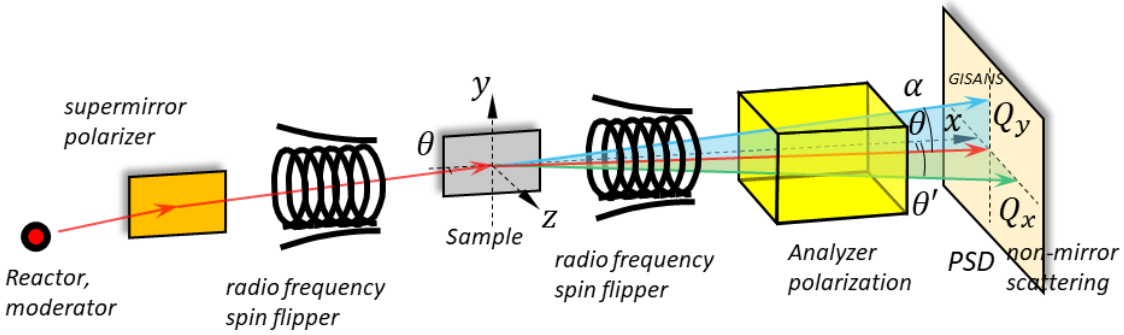

Figure 1: Scheme of reflectometric experiment with full polarization analysis.

In this experiment, polarized neutron spectrometer REMUR in Dubna is being used to characterize heterostructures samples [12]. One feature of reflectometry mode in REMUR reactor is that it has spin-flippers tool which allowed observation of spin asymmetry (SA) that might arise such as in proximity effect of superconductivity. Suppression of ferromagnetism due to

spilling of cooper pair inside ferromagnet could be deduced by comparing spin asymmetry of S/F heterostructures above and below superconducting transition temperatures.

1.3 Aim and methodology

Studying low-dimensional heterostructures made of elements such as sapphire substrate (AL2O3), niobium (Nb), gadolinium (Gd), vanadium (V), and others can help us understand the issues of coexisting superconductivity and ferromagnetism. Figure 2, utilizing the X-ray and polarized neutron reflectometry numerical models. The primary responsibilities involve utilizing Spectra Viewer software to process the experimental data spectra, fitting data to a physical model using MATLAB software, and modeling the reflectivity curve based on various parameters. Several software programs were used in this project to compute and simulate numerical data. For example, Spectra Software was used to open and extract numerical data from the neutron reflectometry experiment. The X-Ray reflectivity from heterostructure layers was simulated using the X'Pert Reflectivity program. Furthermore, simulation and numerical computation of neutron reflectivity were carried out by MATLAB using Lemur.m file provided by Dr. Vladimir. Finally, plotting and several calculations were carried out using Origin Lab.

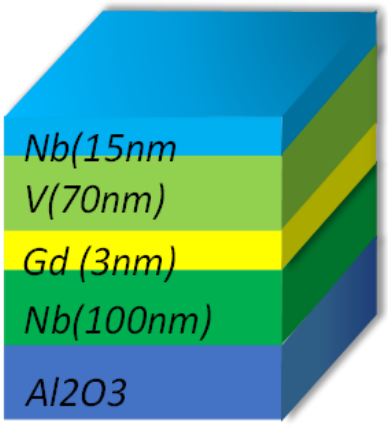

Figure 2: Low dimensional hetero structure.

2. Tasks

2.1 Task 1: fitting experimental data

Using the experimental data of the reflectivity of plus (spin flipper on) and minus (spin flipper off) polarized neutrons, collected by the REMUR spectrometer at two different temperatures (1.5 K below Tc, 12 K above Tc) for the nominal structure [Al2O3 / Nb(100nm) / Gd(3nm) / V(70nm) / Nb(15nm)].

The numerical values of these data were extracted using Spectra Viewer software and exported to Origin Lab. The spin asymmetry was calculated from the experimental data using the following equation:

$$SA = \frac{R_+ - R_-}{R_+ + R_-} \qquad (1)$$

The wavelength of the experimental data was measured by using the following formula:

$$\lambda[\text{Å}] = \frac{(\text{N}+35-12)\cdot 3.956\cdot 256}{34030} \qquad (2)$$

After performing calculation and plotting of experimental data, neutron reflectivity data were compared with the theoretical data resulting from simulation of the same nominal structure in MATLAB, using 6 mrad grazing angle of neutron, the results are shown in **Figure 3**.

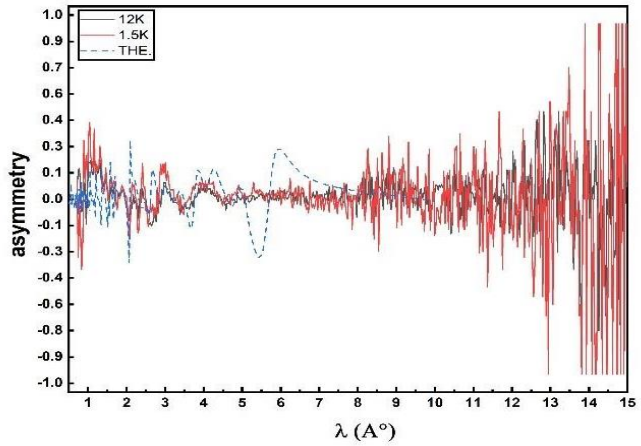

Figure 3: Experimental and Theoretical spin asymmetry at 1.5 K and 12 K.

From figure 3, it can be concluded that spin asymmetry of experimental result and simulation are closely matched and due to differing asymmetry values,

in either case, it was assumed that spin asymmetry value arises in superconductivity layers due to ferromagnetic suppression of Gd layers (inverse proximity effect), and we also notice large variation in the spin asymmetry at the end part of the experimental plot which is due to the small numbers of the neutrons at this range of wavelength (above 10 angstrom) .

2.2 Task 2: Comparing reflectivity at different grazing angles

Based on the following formula, the reflectivity of neutrons is related to the radiation angle.

$$Q = \frac{4\pi}{\lambda}\theta \qquad (3)$$

In this part we examined through simulation how different grazing angles for the beam affects the reflectivity of the neutrons for [Al_2O_3 / Nb(100nm) / Gd(3nm) / V(70nm) / Nb(15nm)] heterostructure with 0 magnetization for all layers (so we expect the graph of plus and minus neutrons to be almost identical due to the absence of magnetization), and we compare reflectivity at grazing angles $\theta = 3,\ 6,\ 12$ mrad for that as shown in **Figure 4**.

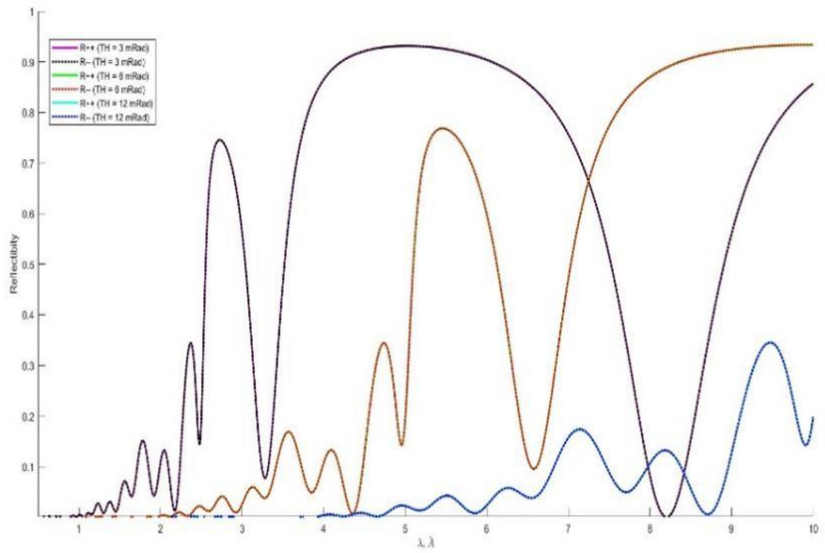

Figure 4: Neutron reflectivity at grazing angles θ = 3, 6, 12 mrad.

From Figure 4, we can observe that the neutrons' momentum is inversely proportional to the incident angle of the neutron beam, Eq.3. So, The peaks

of the graph shift towards larger wavelengths as we increase the grazing angle. In addition, the amplitude of reflectivity tends to decrease as we increase the angle which is attributed to the decreasing of the intensity of the reflected beam by increasing the grazing angle.

Finally, we can notice that the curves corresponding to the "plus" and "minus" reflectivity of neutrons overlap almost exactly for all angles due to the absence of magnetization.

2.3 Task 3: Comparing reflectivity at different magnetization

In this task, we analyzed the dependence of the neutron reflectivity on the strength of magnetization and its direction in the of Gadolinium layer (ferromagnetic layer) for:

:

- Collinear case (magnetization parallel to the sample surface only z direction): M_z (Gd) = 100, 1000, 10000 Oe; M_x (Gd)=0, M_y (Gd)=0

- Non-collinear case: Mx (Gd) = 100, 500, 1000 Oe; Mz (Gd)=1000 Oe, M_y (Gd)=0, the results related to this problem are presented as follows in figure 5 and figure 6:

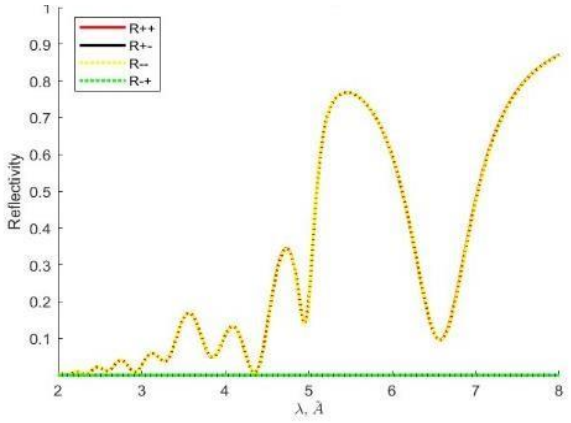

(a) (Mx, My, Mz) = (0, 0, 100)

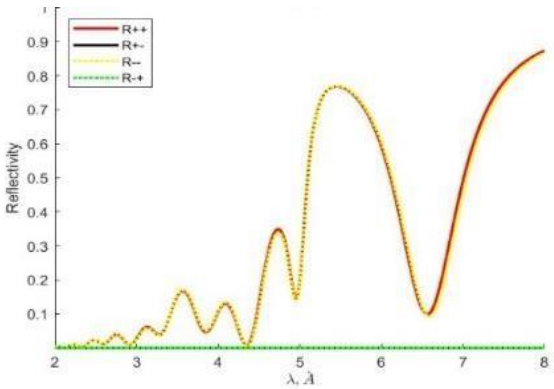

(b) (Mx,My, Mz) = (0, 0, 1000)

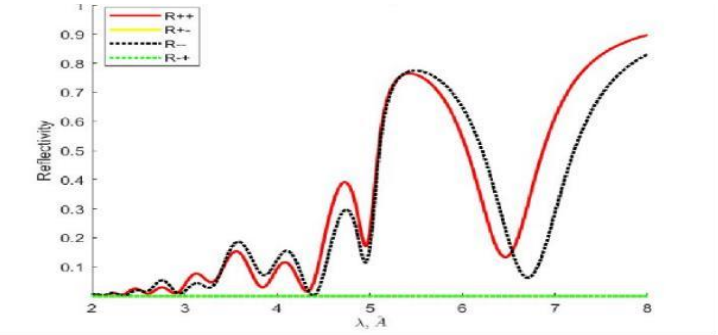

(c) (Mx, My, Mz) = (0, 0, 10000)

Figure 5: (a, b, c) Collinear magnetization.

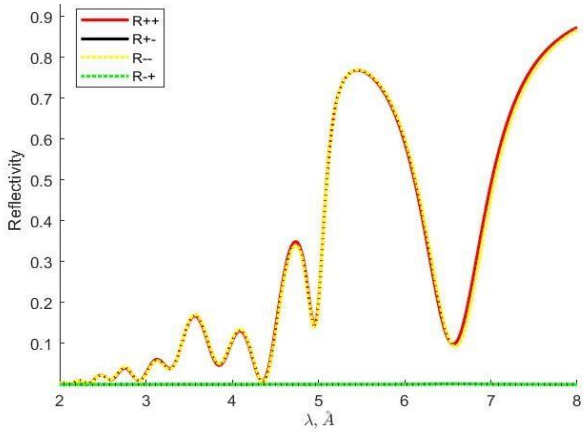

(d) (Mx, My, Mz) = (100, 0, 1000)

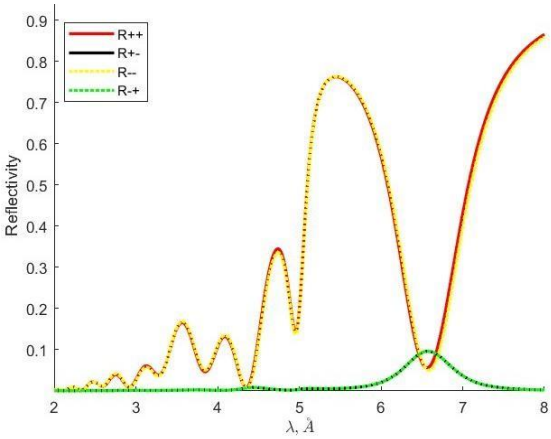

(e) (Mx, My, Mz) = (1000, 0, 1000)

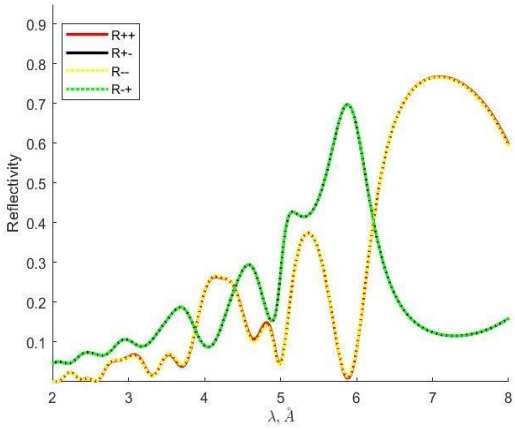

(f) (Mx, My, Mz) = (10000, 0, 1000)

Figure 6: (d, e, f) non-collinear magnetization.

Figure 5 for the collinear case shows that the difference between (plus and minus neutrons) becomes more prominent and apparent as the strength of

magnetization increases $M_{z\ only}$ (M_X =0 and M_y = 0) which is justifiable as the two neutron kinds differ by a magnetic property. Whereas figure **6** represents the non-collinear case for M_z=1000 Oe and M_x changes from 100 to 10000 Oe where there is no change in the reflectivity graphs.

It can be concluded that the polarized neutrons that have occurred remain constant. In addition, by increasing M_x the neutron spin flip will increase, and peaks appear. It is worth mentioning that until M_x=1000, Spin Flips were zero.

2.4 Task 4: Comparing structures with different thickness (calculation of neutron and X-ray reflectivity)

The third parameter which we analyzed is the thickness of the ferromagnetic layer of Gd. The calculation is performed for 12, 30, and 60 nm thick at the same grazing angle in the absence of any form of magnetization. Due to the coherence, length of superconductivity, this layer mustn't be too thick. The depth of the penetration of the superconductivity can be a few nanometers in the ferromagnetic layer. We have observed how reflectivity is influenced. However, we measure the reflectivity for both the neutrons (plus and minus) and a simulated X-ray spectrometer for the same sample as shown in figure 7 and figure 8.

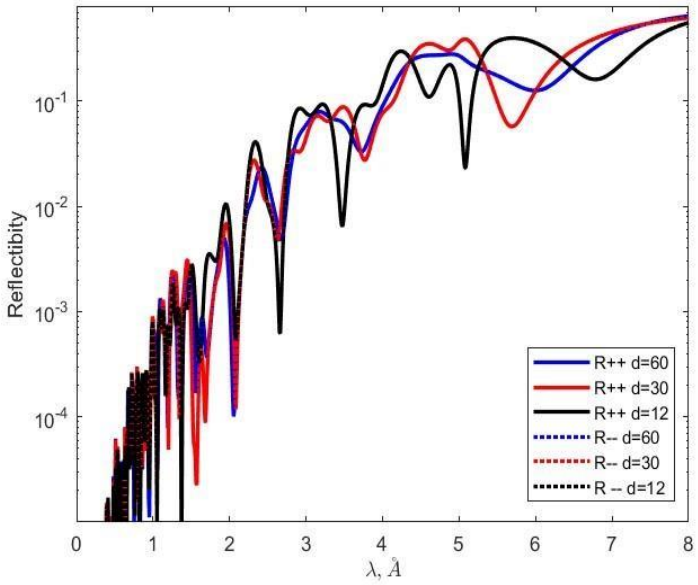

Figure 7: neutron reflectivity of Gd (12, 30, and 60 nm).

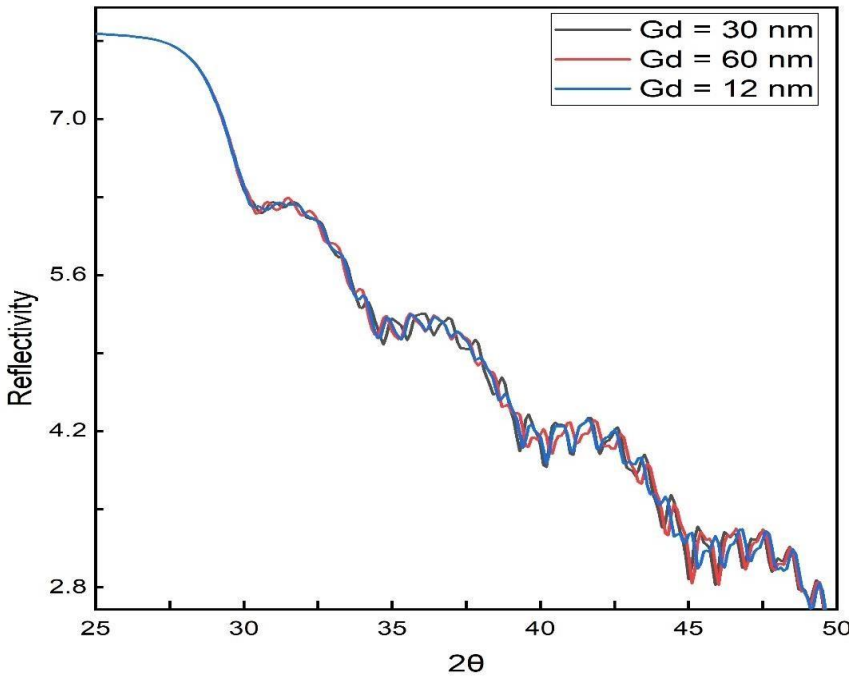

Figure 8 X-ray reflectivity of Gd (12, 30, and 60 nm).

First, it can be concluded from figure 7 that with the increase in the thickness of the Gd layer, the reflectivity also decreases, so that the maximum peak with a thickness of 3 nm is almost 2 times the maximum peak reflectivity with a thickness of 12 nm.

The reduction in neutron reflectivity with increasing thickness can be attributed to the fact that a higher thickness causes the superconducting order parameter within Gd to reach a deeper region. Consequently, more electrons in superconductors are correlated with cooper pairs due to Cooper pair coherence. Consequently, the superconducting layer thickness, filtering the ferromagnetic response of the Gd layer. Also, since we are aware that increasing thickness did not alter beam interaction with the heterostructures, there were no plus or negative variations seen in the neutron beam simulation.

On the other hand, X-ray reflectivity does not change much by increasing the thickness of Gd layer in figure 8. Which is acceptable as the Gd layer in the middle of heterostructures does not contribute much to X-ray scattering as it mainly occurred at the surface. Since we know that X-Ray does not penetrate deeply inside metal then we could safely add more thickness of Gd layer.

However, the intensity of X-ray reflectivity tends to decrease by increasing the incident angle.

2.5 Task 5: Comparing structures with different ferromagnets (calculation of neutron and X-ray reflectivity)

The reflectivity of the neutron, as well as X-Ray, were simulated with variations of ferromagnetic layers for following structures:

Al2O3 / Nb(100nm) / Gd(3nm) / V(70nm) / Nb(15nm)

Al2O3 / Nb(100nm) / Fe(3nm) / V(70nm) / Nb(15nm)

Al2O3 / Nb(100nm) / Co(3nm) / V(70nm) / Nb(15nm)

There were no magnetizations, and the grazing angle was constant = 6 mrad, the results are shown in figure **9** and figure 10.

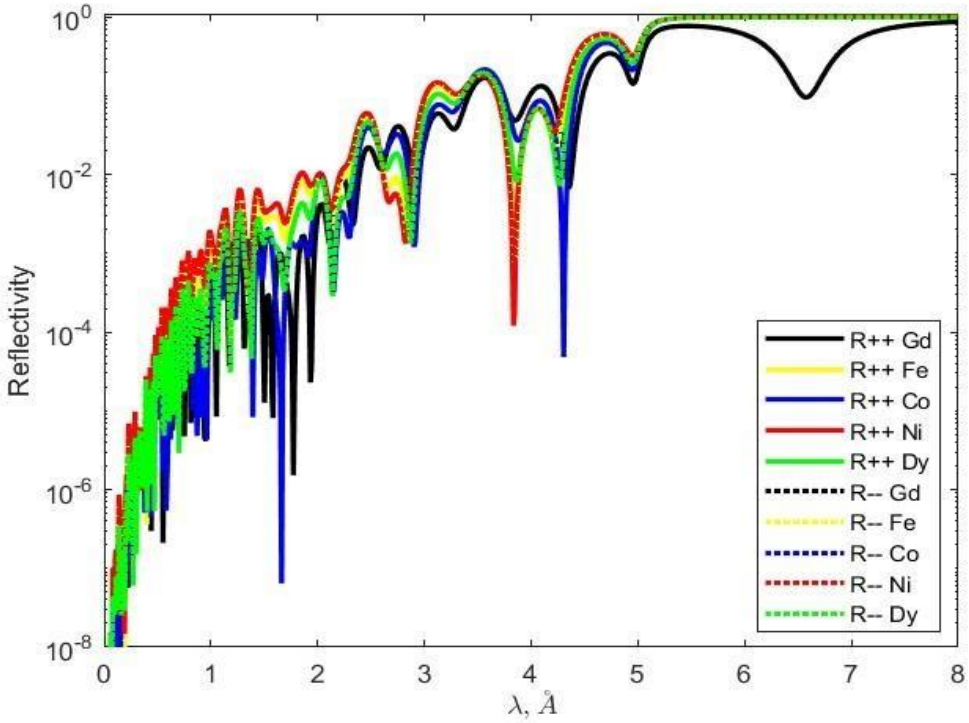

Figure 9 Neutron reflectivity for GD, Fe, Ni, Co, Dy(3nm)

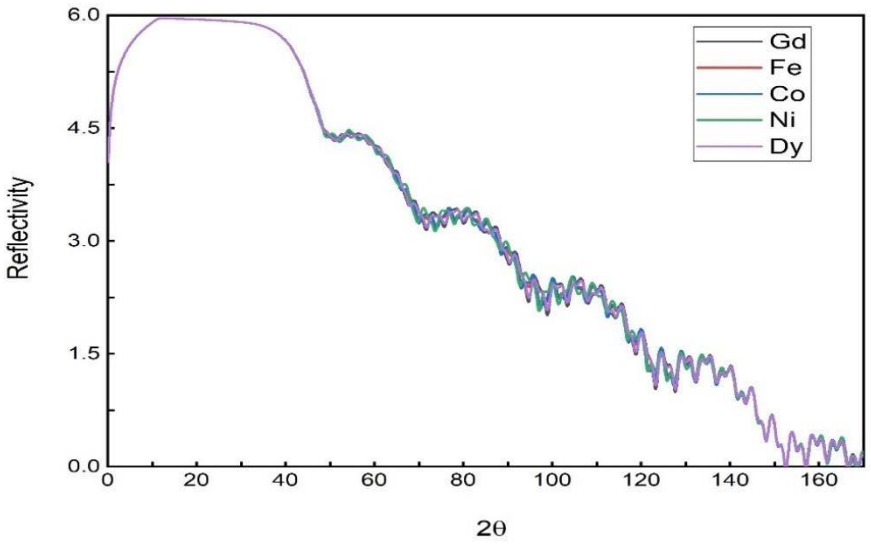

Figure 10 X-ray reflectivity for GD, Fe, Ni, Co, Dy(3nm)

The simulations show that neutron reflectivity has variational reflectivity in each peak of the upper left in figure 9. Variational reflectivity below 5 Angstrom happened because ferromagnetism in the layer had various magnetic moment values. As such it has a differing effect on the proximity effect in superconductivity. Gd has a different neutron reflectivity value because in Gd/Nb layer, Er ~ Es and as such allow rather a large proximity effect where Gd has superconductivity inside it.

As a result, it screened out incoming neutrons and has lower reflectivity. On the other hand, there is no change in the X-ray reflectivity due to elemental variations. As explained previously, this can be attributed to the location of the elements which were in the middle of heterostructures, and because of that, it did not contribute significantly to x-ray scattering.

2.6 Task 6: Superlattice (calculation of neutron and X-ray reflectivity)

In this task, we evaluated the reflectivity changing for the determined superlattices of this specific layer coupling by coupling Gd (ferromagnetic) and Nb (superconductor) elements as a specific layer and repeating them several times. we have drawn the graph of the changes X-Ray and Neutron reflectivity for the following structures:

Al2O3 / [Nb(25nm) / Gd(3nm)] x10 / Nb(15nm)

Al2O3 / [Nb(25nm) / Gd(3nm)] x20 / Nb(15nm)

Al2O3 / [Nb(25nm) / Gd(3nm)] x30 / Nb(15nm)

There were no Magnetizations and θ = 6 mrad, the results related to this problem are presented in figure 11 and figure 12.

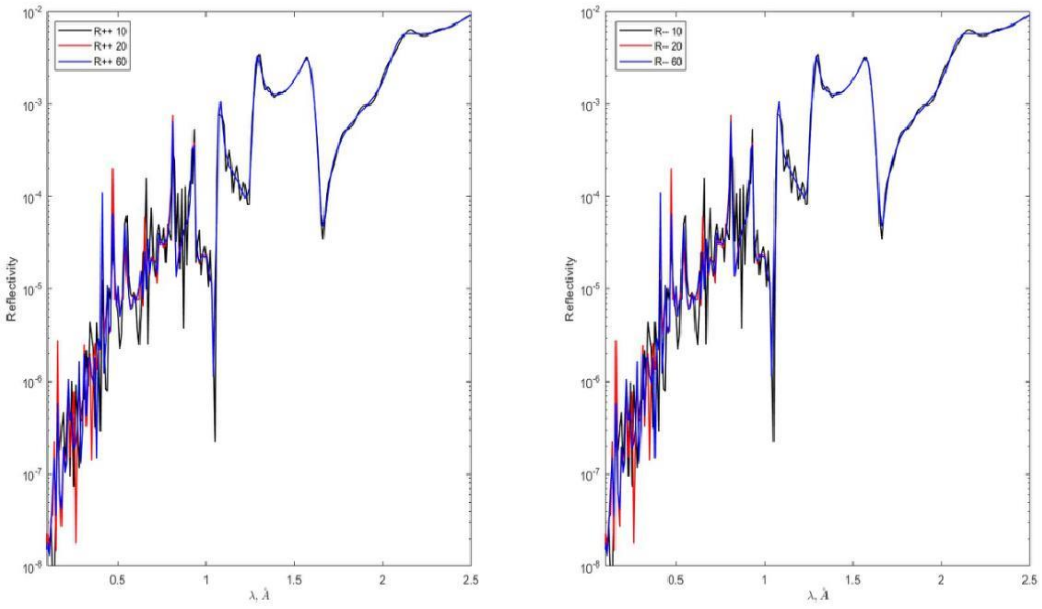

Figure 11: Calculation of neutron for [Nb(25nm) / Gd(3nm)] x10, 20, 30

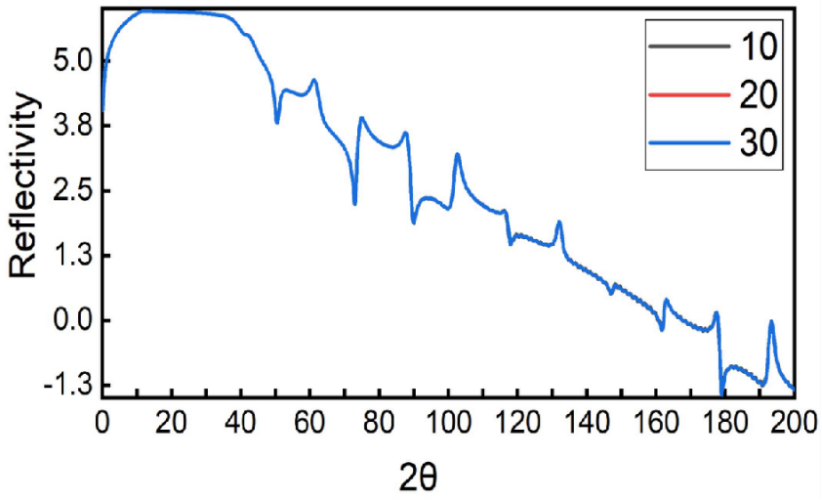

Figure 12: Calculation of X-Ray for [Nb(25nm) / Gd(3nm)] x10, 20, 30

According to figure 11, it can be concluded that the more the number of pairs of layers increases, the intensity of the neutron reflectivity also increases.

Figure 12 illustrates that as the number of layers is increased, the X-ray intensity does not alter. This is explained by the fact that, for a material with a high surface electronic density of states, such transition metal, the X-ray penetration depth was rather shallow. Since neutrons have a deeper penetration than X-rays, the inclusion of more heterostructure layers resulted in a higher value of neutron reflectivity. To predict a greater nuclear magnetic moment that could scatter neutrons as we add more layers to the samples.

2.7 Task 7: Influence of roughness (calculation only X-ray reflectivity)

The penetration of X-ray beams in metallic material is small so it interacts on the surface, and we can discuss the roughness of the layers.
The X-ray spectra for different roughness of 0, 1, 2, and 3 nm for the [Al2O3/[Nb(25nm)/Gd(3nm)]$_{20}$/Nb(15nm)] heterostructure are shown in figure 13.

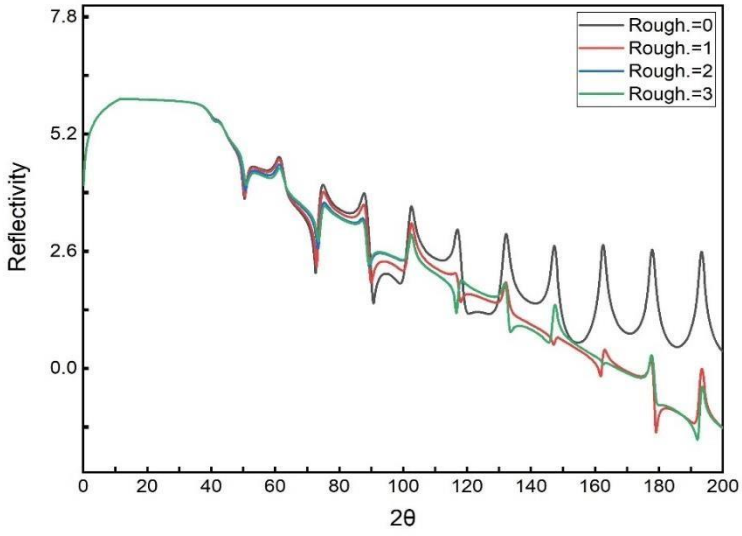

Figure 13. X-ray reflectivity for investigated heterostructures with the roughness of Gd layer of 0, 1, 2, and 3 nm.

From figure 13, we can observe that with the increase in roughness, the peaks and fluctuations of the graph related to the X-ray intensity for different incident angels decrease and the graph looks smoother, this can be explained by X-ray scattering experiments which often relied on the fact that detectors could only detect scattered beams that arrived at it, including superposition of beam due to lattice scattering of multilayers samples.

2.8 Task 8: Structure with helicoidal magnetic (calculation only of neutron reflectivity)

In this task, we studied the variation of the reflectivity for the Dy element with helicoidally magnetic properties, we have drawn the diagram of neutron reflectivity changes for M_z=Mx=100, Structure with helicoidally magnetic by calculation only of neutron reflectivity for following structure:

Al2O3 / Nb(100nm) / Dy(3nm) / V(70nm) / Nb(15nm)

And Separate Dy-layer to 20 sublayers, with Mz and Mx modulate helicoid The figure of the results related to this problem are presented in figure 14:

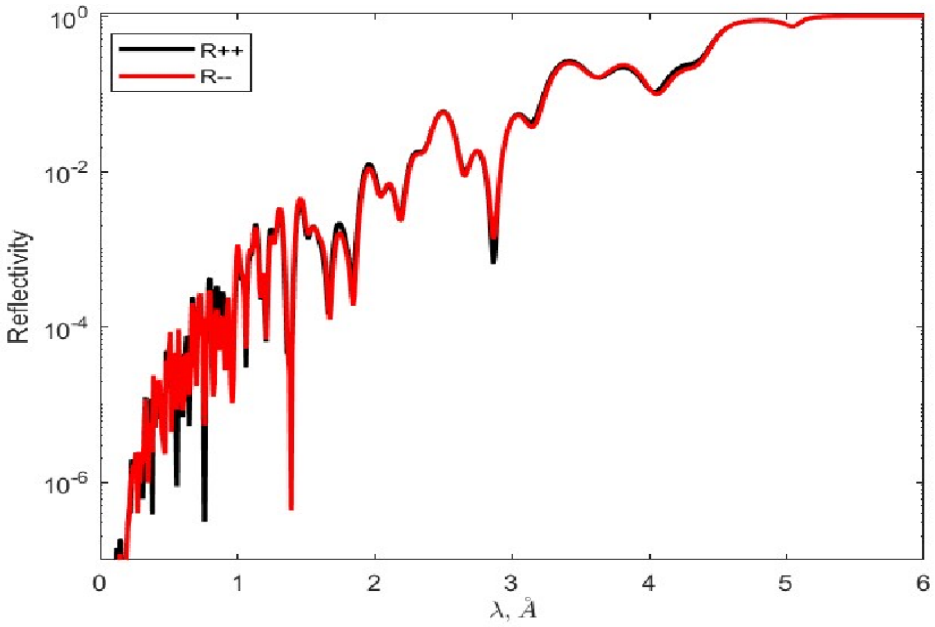

Figure 14: Neutron reflectivity for Mx, Mz (Dy)=1000 Oe

From figure 14, we noticed that the separation between plus and minus beams is apparent for small values of magnetization, and it will be more apparent for the larger magnetization magnitude.

References

[1] P. F. Dahl, “Kamerlingh Onnes and the Discovery of Superconductivity: The Leyden Years, 1911-1914,” *Historical Studies in the Physical Sciences*, vol. 15, no. 1, pp. 1–37, Jan. 1984,

[2] V. L. Ginzburg, “Nobel Lecture: On superconductivity and superfluidity (what I have and have not managed to do) as well as on the ‘physical minimum’ at the beginning of the XXI century,” *Rev Mod Phys*, vol. 76, no. 3, pp. 981–998, Dec. 2004,

[3] P. G. de GENNES, “Boundary Effects in Superconductors,” *Rev Mod Phys*, vol. 36, no. 1, pp. 225–237, Jan. 1964,

[4] V. L. Aksenov, Yu. v. Nikitenko, A. v. Petrenko, V. M. Uzdin, Yu. N. Khaidukov, and H. Zabel, “Features of the magnetic state of the layered Fe-V nanostructure of the superconductor-ferromagnet type,” *Crystallography Reports*, vol. 52, no. 3, pp. 381– 386, May 2007,

[5] Yu. N. Khaydukov *et al.*, “Magnetic and superconducting phase diagram of Nb/Gd/Nb trilayers,” *Phys Rev B*, vol. 97, no. 14, p. 144511, Apr. 2018,

[6] Z. Radovic, M. Ledvij, L. Dobrosavljevic -Grujic, A. I. Buzdin, and J. R. Clem, “Transition temperatures of superconductor-ferromagnet superlattices,” 1991. [Online].

[7] Y. N. Proshin and M. G. Khusainov, “Manifestations of the Larkin-Ovchinnikov-FuldeFerrell state in bimetal ferromagnet-superconductor structures,” 1997. [Online].

[8] T. Löfwander, T. Champel, J. Durst, and M. Eschrig, “Interplay of Magnetic and
[9] Superconducting Proximity Effects in Ferromagnet-Superconductor-Ferromagnet Trilayers,” *Phys Rev Lett*, vol. 95, no. 18, p. 187003, Oct. 2005,

[10] A. Rühm, B. P. Toperverg, and H. Dosch, “Super matrix approach to polarized neutron reflectivity from arbitrary spin structures,” *Phys Rev B*, vol. 60, no. 23, pp. 16073–16077, Dec. 1999,

[11] Y. V. Nikitenko and V. D. Zhaketov, “Magnetism in Ferromagnetic-Superconducting Layered Structures,” *Physics of Particles and Nuclei*, vol. 53, no. 6, pp. 1089–1125, Dec. 2022, [Online].

[12] M. Utsuro, V. K. Ignatovich, W. Verlag GmbH, and C. KGaA, “Neutron Optics.”

[13] V. D. Zhaketov *et al.*, “Polarized Neutron Reflectometer with the Recording of Neutrons and Gamma Quanta,” *Journal of Surface Investigation*, vol. 15, no. 3, pp. 549–562, May 2021, [Online].